Journal of Biomedical Optics

SPIEDigitalLibrary.org/jbo

Multiple scattering of polarized light: comparison of Maxwell theory and radiative transfer theory

Florian Voit
Ansgar Hohmann
Jan Schäfer
Alwin Kienle

SPIE

Multiple scattering of polarized light: comparison of Maxwell theory and radiative transfer theory

Florian Voit,* **Ansgar Hohmann,*** **Jan Schäfer, and Alwin Kienle**
Institut für Lasertechnologien in der Medizin und Meßtechnik, Helmholtzstr. 12, D-89081 Ulm, Germany

Abstract. For many research areas in biomedical optics, information about scattering of polarized light in turbid media is of increasing importance. Scattering simulations within this field are mainly performed on the basis of radiative transfer theory. In this study a polarization sensitive Monte Carlo solution of radiative transfer theory is compared to exact Maxwell solutions for all elements of the scattering Müller matrix. Different scatterer volume concentrations are modeled as a multitude of monodisperse nonabsorbing spheres randomly positioned in a cubic simulation volume which is irradiated with monochromatic incident light. For all Müller matrix elements effects due to dependent scattering and multiple scattering are analysed. The results are in overall good agreement between the two methods with deviations related to dependent scattering being prominent for high volume concentrations and high scattering angles. [DOI: 10.1117/1.JBO.17.4.045003]

Keywords: Monte Carlo; Maxwell theory; polarization; multiple scattering; random media.

Paper 11751P received Dec. 14, 2011; revised manuscript received Feb. 15, 2012; accepted for publication Feb. 16, 2012.; published online Apr. 11, 2012.

1 Introduction

The investigation of polarized light propagation in scattering media is an aspiring field in biomedical optics. In many areas of research understanding of light propagation in biological tissue becomes more and more important.[1–3] Polarized light has a high potential in a large variety of diagnostic purposes for gaining morphological and functional information as for example *in-vivo* noninvasive glucose sensing, skin cancer detection and bacteria sensing.[4–6] The establishment of possible polarized light applications and their improvement imply an accurate method for polarized light propagation modeling.

Monte Carlo simulations of light propagation in turbid media are used for the numerical solution of the radiative transfer theory since decades.[7,8] There exists a variety of Monte Carlo programs for a wide range of applications. Though, only a limited number of investigations which describe polarization dependent light propagation in turbid media has been presented. Experimental determination of the Müller matrix elements is well-known[9–13] and also different simulation approaches using the Monte Carlo method have been published.[10,13–21] However, this commonly used approach is an approximation compared to accurate solutions based on Maxwell theory.

An alternative approach is the solution of Maxwell's equations. In general, Maxwell theory provides exact solutions, but mostly requires much more computer resources since, apart from a few exceptions, numerical solution methods (e.g., Finite-Difference Time-Domain,[22] Discrete Dipole Approximation[23]) have to be used. The extensive requirements for computational power are the major drawback of these solution methods. Monte Carlo programs generally require less computational power. However, it is quite difficult to assess under which conditions radiative transfer theory is a satisfying approximation of Maxwell theory.

Differences in scattering cross sections calculated by radiative transfer theory and Maxwell theory were described in literature.[24] Schäfer and Kienle[25] showed that there is a good agreement for the angle-dependent differential scattering cross section between the two methods in two-dimensional light propagation problems. A similar agreement was observed for low scatterer concentrations as well.[26] Also in three dimensions it was found[27] that for unpolarized light deviations due to radiative transfer theory remain small, even for concentrations up to about 20 Vol.-% for the investigated sphere diameters. To our knowledge, there is a lack of reference studies so far, which directly compare solutions of Maxwell theory to the radiative transfer theory in case of polarized light.

One goal of this study was to develop a Monte Carlo program (see also Hohmann et al.[28] and Kienle et al.[29]) for simulation of polarized light propagation in three-dimensional turbid media. By using the results from this program for the scattering by multiple spheres and from an appropriate Maxwell solution (Generalized Multisphere Mie, see Xu and Gustafson[30]) direct comparison between the Monte Carlo and Maxwell methods calculating polarized light propagation has been carried out. A further goal of this study was to show the similarities and differences between the two methods using the whole Müller matrix formalism. This was performed by calculating the normalized Müller matrix elements while taking into account different concentrations of scatterers in the simulation medium.

2 Methods

For comparison of the two calculation methods [(1) Monte Carlo method as a numerical solution of the radiative transfer theory and (2) Generalized Multisphere Mie (GMM) as an analytical solution of Maxwell theory], a certain number (12, 24, 48 or 96) of scattering spheres (radius $r = 1\ \mu$m) was assumed to

*A. Hohmann and F. Voit contributed equally to this work.

Address all correspondence to: Alwin Kienle, Institut für Lasertechnologien in der Medizin und Meßtechnik, Helmholtzstr. 12, D-89081 Ulm, Germany. Tel: +49 7311429224; E-mail: alwin.kienle@ilm.uni-ulm.de.

0091-3286/2012/$25.00 © 2012 SPIE

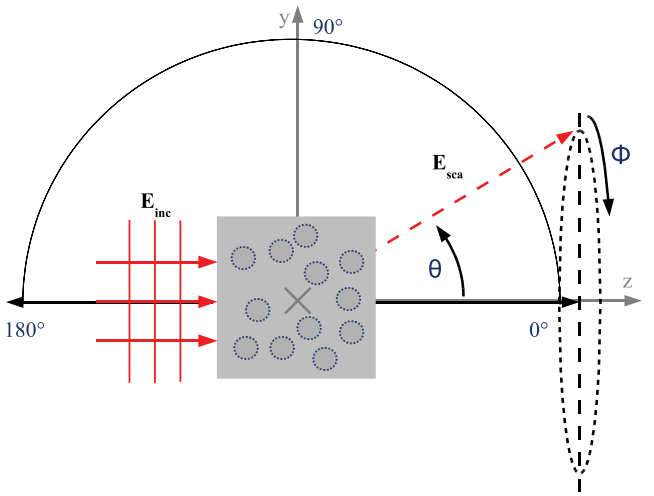

Fig. 1 Scattering scene of the multiple sphere model. Incident light ($\mathbf{E}_{inc}$) enters a cubic simulation volume from where it is scattered to all angular directions ($\mathbf{E}_{sca}$). For illustration the orientations of scattering angle θ and azimuthal angle ϕ are shown.

be randomly distributed in a cubic simulation volume with an edge length of $D = 10\ \mu$m. This simulation volume was irradiated perpendicularly to one side by a plane monochromatic wave (wavenumber k) and the scattered light was registered at a far-field distance r, $r \gg D$, from the origin of the simulation volume for each scattering angle θ and azimuthal angle ϕ. By this approach, the polarization-dependent scattering characteristics of the whole sphere distribution can be calculated and described by the so-called Müller matrix.[31] To reduce the statistical noise the results were averaged over all azimuthal angles ϕ for both methods. This Müller matrix describes the transformation of the polarization state characterized by the Stokes vector $\mathbf{S}^{st} = (I, Q, U, V)^T$ from its incident state $\mathbf{S}_i^{st}(\theta)$ to its final state $\mathbf{S}_f^{st}(\theta)$ through the scattering system[32] [see Eq. (1) and Fig. 1].

$$\mathbf{S}_f^{st}(\theta) = \frac{1}{k^2 r^2} \begin{pmatrix} S_{11}(\theta) & S_{12}(\theta) & S_{13}(\theta) & S_{14}(\theta) \\ S_{21}(\theta) & S_{22}(\theta) & S_{23}(\theta) & S_{24}(\theta) \\ S_{31}(\theta) & S_{32}(\theta) & S_{33}(\theta) & S_{34}(\theta) \\ S_{41}(\theta) & S_{42}(\theta) & S_{43}(\theta) & S_{44}(\theta) \end{pmatrix} \mathbf{S}_i^{st}(\theta). \tag{1}$$

2.1 *Monte Carlo Model*

A Monte Carlo program for simulation of polarized light propagation in scattering media was developed based on the radiative transfer theory.[10,13,15–18,20,21,28] The Monte Carlo method simulates a multitude of random light propagation paths through the medium omitting the wave character of light, nonetheless considering polarization effects. The scatterers were assumed to be randomly distributed within a simulation volume of $V = 10 \times 10 \times 10\ \mu\text{m}^3$ and to have an angularly-resolved scattering probability (phase function) similar to the phase function of a single sphere.

This phase function was calculated using Mie theory (single homogeneous sphere in a homogeneous medium, see Bohren and Huffman[32] and Mie[33]) and used in case of a scattering event. For polarized light, this phase function depends on both the scattering angle as well as on the polarization state of the incident light. The optical properties of polystyrene microspheres (radius $r = 1\ \mu$m) in water were used as input parameters for the spherical scatterers in the Mie program: the refractive index of the spheres was $n = 1.59$ in an infinite medium of $n_m = 1.33$. There was no difference between the refractive index of the medium within the simulation volume and the surrounding medium. The vacuum wavelength of the light was set to $\lambda = 600$ nm. This results in a size parameter $x = 2\pi r n_m/\lambda \approx 13.928$.

The scattering efficiency $Q_{sca} = C_{sca}/(\pi r^2)$ of a single sphere resulting from the Mie program can be applied to calculate the scattering coefficient μ_s as in Eq. (2) used for the Monte Carlo simulations

$$\mu_s = f_V \cdot \frac{C_{sca}}{V_s} = \frac{N \cdot V_s}{V} \cdot \frac{C_{sca}}{V_s} = \frac{N}{V} \cdot Q_{sca} \cdot \pi r^2, \tag{2}$$

where the volume of a single sphere V_s, the scattering cross section C_{sca} and the volume fraction (concentration) f_V of N spheres in a volume V are given. A volume fraction f_V of 5.03 Vol.-% (corresponding to a number of spheres $N = 12$), 10.05 Vol.-% ($N = 24$), 20.11 Vol.-% ($N = 48$) and 40.21 Vol.-% ($N = 96$) resulted in a scattering coefficient of $\mu_s = 111.73\ \text{mm}^{-1}$, $\mu_s = 223.46\ \text{mm}^{-1}$, $\mu_s = 446.91\ \text{mm}^{-1}$ and $\mu_s = 893.82\ \text{mm}^{-1}$, respectively, for the Monte Carlo simulations. The absorption coefficient was set to zero for all concentrations. The number of photons used for the simulations was $3 \times 10^8 (N = 12, 24, 48)$ and $1 \times 10^8 (N = 96)$, respectively.

A commonly used technique to gain the Müller matrix elements of a scatterer system via the Monte Carlo method is the subsequent execution of four simulations applying an incident Stokes vector $\mathbf{S}_i^{st}$ of $(1,1,0,0)^T$, $(1,-1,0,0)^T$, $(1,0,1,0)^T$ and $(1,0,0,1)^T$ which is labeled by H, V, P and R, respectively.[6,20] The exit (scattering) angle of each photon which left the simulation volume was registered for each simulation run together with its corresponding Stokes vector. The results are four scattered Stokes vectors $\mathbf{S}_f^{st}$: $(I_H, Q_H, U_H, V_H)^T$, $(I_V, Q_V, U_V, V_V)^T$, $(I_P, Q_P, U_P, V_P)^T$ and $(I_R, Q_R, U_R, V_R)^T$. These four Stokes vectors, resulting from the average of many photon paths, can be used to calculate the Müller matrix of the system:

$$\frac{1}{k^2 r^2} \begin{pmatrix} S_{11} & S_{12} & S_{13} & S_{14} \\ S_{21} & S_{22} & S_{23} & S_{24} \\ S_{31} & S_{32} & S_{33} & S_{34} \\ S_{41} & S_{42} & S_{43} & S_{44} \end{pmatrix} = \frac{1}{2} \begin{pmatrix} I_H + I_V & I_H - I_V & 2I_P - I_H - I_V & 2I_R - I_H - I_V \\ Q_H + Q_V & Q_H - Q_V & 2Q_P - Q_H - Q_V & 2Q_R - Q_H - Q_V \\ U_H + U_V & U_H - U_V & 2U_P - U_H - U_V & 2U_R - U_H - U_V \\ V_H + V_V & V_H - V_V & 2V_P - V_H - V_V & 2V_R - V_H - V_V \end{pmatrix}. \tag{3}$$

By this method, the angular distribution of each Müller matrix element was obtained. All Müller matrix elements were normalized to the S_{11} element for each scattering angle θ and the Müller matrix element $S_{11}(\theta)$ was normalized to the $S_{11}(0)$ element for all angles θ. The resulting normalized Müller matrix is denoted by $\mathbf{M}$ in Sec. 3.

2.2 *Maxwell Theory*

A Maxwell solution for the scattering problem is given by the Generalized Multiparticle Mie approach, an extension of Mie theory, which is able to handle multiple spherical scatterers and, as an exact solution, also takes into account dependent scattering effects. A Fortran code is provided by Xu et al.[34] and used as a reference Maxwell solver. Therein the scattering of an incident plane wave by a distinct arrangement of spheres is calculated by employing the wave equation as opposed to the statistical Monte Carlo model dealing with photon paths.

The total scattered field results from coherent superposition of the scattered field contributions $\mathbf{E}_{\text{sca}}^{j}$ of each sphere j:

$$\mathbf{E}_{\text{sca}} = \sum_{j} \mathbf{E}_{\text{sca}}^{j}. \tag{4}$$

Therein the field $\mathbf{E}_{\text{sca}}^{j}$ scattered by each individual sphere results from an incident field $\mathbf{E}_{\text{inc}}^{j}$ which is composed of the external incident field $\mathbf{E}_{\text{inc},0}^{j}$ as well as the scattered fields from all other spheres:

$$\mathbf{E}_{\text{inc}}^{j} = \mathbf{E}_{\text{inc},0}^{j} + \sum_{k,k\neq j} \mathbf{E}_{\text{sca}}^{k,j}. \tag{5}$$

The solution of the resulting equation system is described in detail by Xu.[30] It yields expansion coefficients for the scattered field containing interaction information of the whole sphere arrangement. This is referred to as dependent scattering. In the far-field, a (2×2) complex-valued amplitude scattering matrix $\mathbf{S}(\theta,\phi)$ can be derived[35] for monochromatic incident light which specifies the angular part of the scattered spherical wave's amplitude distribution. Thus, the scattering problem can be compactly written as[32]

$$\mathbf{E}_{\text{sca}} = \frac{e^{ik(r-z)}}{-ikr} \begin{pmatrix} S_2 & S_3 \\ S_4 & S_1 \end{pmatrix} \mathbf{E}_{\text{inc}}, \tag{6}$$

where the incident plane wave (wavenumber k) propagates along the z-axis (see Fig. 1) and the scatterer is located at the origin of the reference frame. For a given scatterer orientation, all elements $S_1, \ldots, S_4$ of this amplitude scattering matrix in Eq. (6) are generally dependent on scattering angle θ as well as azimuthal angle ϕ. In this formulation, the incident and scattered fields $\mathbf{E} = (E^{\parallel}, E^{\perp})^T$ consist of parallel and perpendicular components which contain all phase information. Yet, these quantities are sophisticated to interpret in terms of polarized intensities as given in the Stokes vector components. Therefore the elements of the amplitude scattering matrix are converted to particular Müller matrix elements $S_{ij}(\theta,\phi), (i,j=1,\ldots,4)$ as can be found in Bohren and Huffman:[32]

$$\begin{aligned}
S_{11} &= \frac{1}{2}\left(|S_1|^2 + |S_2|^2 + |S_3|^2 + |S_4|^2\right) \\
S_{12} &= \frac{1}{2}\left(|S_2|^2 - |S_1|^2 + |S_4|^2 - |S_3|^2\right) \\
S_{13} &= \mathrm{Re}(S_2 S_3^* + S_1 S_4^*) \\
S_{14} &= \mathrm{Im}(S_2 S_3^* - S_1 S_4^*) \\
S_{21} &= \frac{1}{2}\left(|S_2|^2 - |S_1|^2 - |S_4|^2 + |S_3|^2\right) \\
S_{22} &= \frac{1}{2}\left(|S_2|^2 + |S_1|^2 - |S_4|^2 - |S_3|^2\right) \\
S_{23} &= \mathrm{Re}(S_2 S_3^* - S_1 S_4^*) \\
S_{24} &= \mathrm{Im}(S_2 S_3^* + S_1 S_4^*) \\
S_{31} &= \mathrm{Re}(S_2 S_4^* + S_1 S_3^*) \\
S_{32} &= \mathrm{Re}(S_2 S_4^* - S_1 S_3^*) \\
S_{33} &= \mathrm{Re}(S_1 S_2^* + S_3 S_4^*) \\
S_{34} &= \mathrm{Im}(S_2 S_1^* + S_4 S_3^*) \\
S_{41} &= \mathrm{Im}(S_2^* S_4 + S_3^* S_1) \\
S_{42} &= \mathrm{Im}(S_2^* S_4 - S_3^* S_1) \\
S_{43} &= \mathrm{Im}(S_1 S_2^* - S_3 S_4^*) \\
S_{44} &= \mathrm{Re}(S_1 S_2^* - S_3 S_4^*).
\end{aligned} \tag{7}$$

Just like the amplitude matrix, all Müller matrix elements in Eq. (7) depend on both scattering angle θ and azimuthal angle ϕ. Thus, to comply with the θ-dependent Monte Carlo results, each element is azimuthally averaged. In addition, all Müller matrix elements except $S_{11}(\theta)$ itself are normalized to $S_{11}(\theta)$ to get results within a range of $[-1,\ldots,+1]$. For ease of comparison, the intensity $S_{11}(\theta)$ is normalized to the $S_{11}(0)$ Monte Carlo solution.

Since multiparticle Mie theory requires definitely positioned scatterers of finite extent for solution of the underlying boundary conditions, a collection of spheres is randomly distributed in a given simulation volume in order to achieve defined volume concentrations. To approximate homogeneous turbid media models, several random configurations of finite spheres (realizations) are generated where the results are averaged over these realizations. The spheres are randomly distributed under the restriction that no overlapping is allowed. For generation of these distributions a Metropolis shuffling algorithm[36,37] was programmed where each sphere in an initial periodic arrangement (simple cubic lattice) is randomly shuffled many times considering periodic boundary conditions with respect to the cubic volume. This algorithm converges to an equilibrium distribution when performing a high number of displacement steps.

In order to improve convergence of the algorithm, the random step size is adjusted dynamically. An initial displacement step size is randomly chosen within a size interval in the order of the sphere radius. After shuffling each sphere for a predefined number of times, an acceptance rate of allowed (non-overlapping) with respect to tried sphere displacements is evaluated. In case the new position would lead to sphere overlap the tried displacement is rejected and the old position is kept.[37] A small acceptance rate indicates a poor probability to find allowed positions, then the step size is decreased for the next shuffling pass. On the other hand, a high acceptance

rate indicates too small deviation from the initial arrangement, in that case the step size is increased for the next shuffling pass. Generation of sufficiently randomized sphere distributions is achieved if the acceptance rate stays around 50%.

For the Maxwell simulations, the same parameters as for the Monte Carlo simulations were used, i.e., the different volume concentrations are modeled by $N = 12, 24, 48$ and 96 spheres ($r = 1\ \mu$m), respectively, in a simulation volume of $10 \times 10 \times 10\ \mu\text{m}^3$. This volume size allows simulations to be performed in a reasonable amount of time even at higher volume concentrations. Apart from diffraction around forward scattering angles, the characteristics of an infinite scattering medium are reproduced in this subset simulation volume. For the four concentrations 10 distinct random realizations were generated where each sphere is shuffled ca. 10000 times. From these realizations the resulting Müller matrix elements are averaged to reduce interference effects. As above, the incident vacuum wavelength is set to $\lambda = 600$ nm, the relative refractive index to $m = 1.59/1.33$ resulting in a size parameter $x \approx 13.928$.

2.3 *Properties of the Müller Matrix*

Both introduced methods are based on scatterers of spherical symmetry. This leads to a reduction in the number of independent Müller matrix elements. Moreover, random orientation of these scatterers has an additional impact on the matrix properties. For example, arbitrarily shaped scatterers of random orientation lead to 10 independent elements. Employing scatterers which have a plane of symmetry further reduces the number of independent elements to 6 (see van de Hulst[38]). In case of randomly arranged spheres (labeled rs), the Müller matrix can be denoted as

$$\mathbf{S}^{rs} = \begin{pmatrix} a_1 & b_1 & 0 & 0 \\ b_1 & a_2 & 0 & 0 \\ 0 & 0 & a_3 & b_2 \\ 0 & 0 & -b_2 & a_4 \end{pmatrix}. \tag{8}$$

The off-diagonal elements S_{13}^{rs}, S_{14}^{rs}, S_{23}^{rs}, S_{24}^{rs}, S_{31}^{rs}, S_{32}^{rs}, S_{41}^{rs} and S_{42}^{rs} vanish. Further, the elements S_{12}^{rs} and S_{21}^{rs} are symmetric (b_1) whereas S_{34}^{rs} and S_{43}^{rs} are antisymmetric (b_2). All diagonal elements $a_i (i = 1, \ldots, 4)$ are differing. Note that in case of spheres additional relations[38,39] ($a_1 = a_2$, $a_3 = a_4$) are only valid if multiple scattering is neglected (single scattering). That means, multiple scattering can be interpreted as violation of spherical symmetry of an equivalent single scatterer.[6] These diagonal elements a_i characterize the coupling of equal Stokes components by the scattering system. The element b_1 shows the degree of parallel linear polarization with respect to unpolarized incident light whereas b_2 shows the transformation of oblique linear to circular polarization. From the Müller matrix elements information on the conservation of interference effects[40] and polarization states[41] can be derived. For spheres with high relative refractive index it is known that depending on the scatterers' size parameter residing in Rayleigh or Mie regime, linear or circular polarization states are better maintained, respectively.[5,42]

3 Results and Discussion

The resulting 16 angularly resolved Müller matrix elements were compared between the Monte Carlo method and the Maxwell method. Figure 2 shows all angularly resolved Müller matrix elements in case of 24 randomly distributed spheres corresponding to a volume concentration $f_V = 10.05$ Vol.-%. It is obvious that both 2×2 submatrices on the secondary diagonal [see Eq. (8), namely the $M_{13}, M_{14}, M_{23}, M_{24}, M_{31}, M_{32}, M_{41}$ and M_{42} elements] show noisy results around zero for all angles. This behavior was expected for single as well as for multiple scattering by randomly distributed spheres.[38] Further, the well-known symmetry between the M_{12} and M_{21} elements as well as antisymmetry between the M_{34} and M_{43} elements was reproduced by both methods. The remaining concentrations of 12 ($f_V = 5.03$ Vol.-%), 48 ($f_V = 20.11$ Vol.-%) and 96 spheres ($f_V = 40.21$ Vol.-%) dispersed in the medium showed the same expected behavior as above. Because of that, only the relevant Müller matrix elements M_{11}, M_{22}, M_{33}, M_{44} and M_{21},

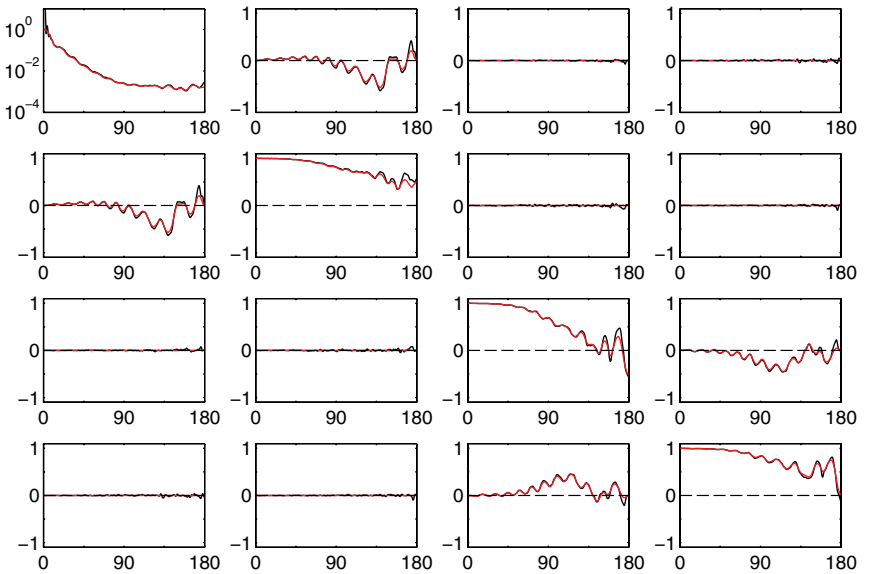

Fig. 2 Angularly resolved Müller matrix: Monte Carlo results (red) and Maxwell results (black) compared to each other. Parameters used: $N = 24$ nonabsorbing spheres (radius $r = 1\ \mu$m, relative refractive index $m = 1.59/1.33$), size of cubic scattering volume $10 \times 10 \times 10\ \mu\text{m}^3$ (volume concentration $f_V = 10.05$ Vol.-%), wavelength of incident light $\lambda = 600$ nm *in vacuo*. All elements are normalized to M_{11}, the M_{11} element is normalized to forward direction. Every element is depicted versus the scattering angle θ in the range from 0 to 180 deg.

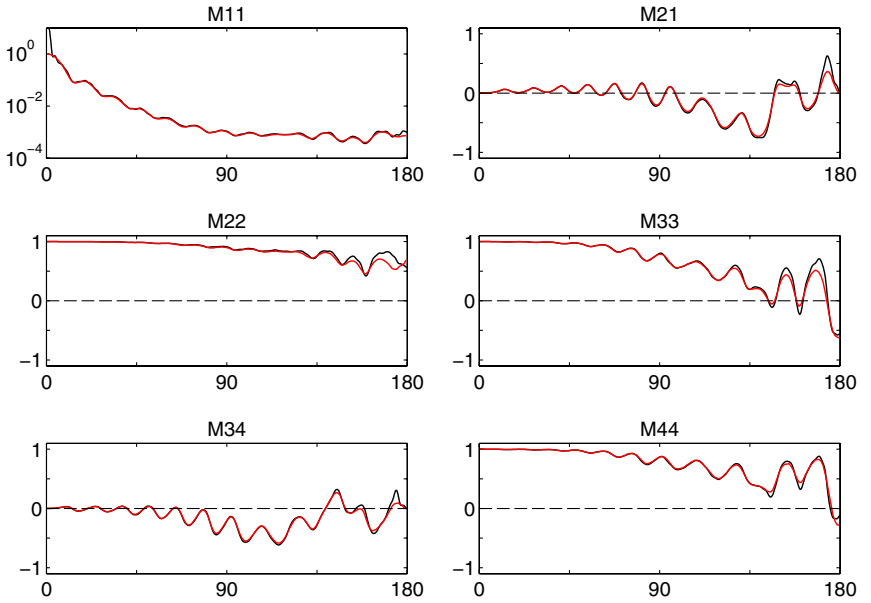

Fig. 3 Relevant Müller matrix elements for $N = 12$ nonabsorbing spheres ($f_V = 5.03$ Vol.-%). All elements are normalized to M_{11}, the M_{11} element is normalized to forward direction. Every element is depicted versus the scattering angle θ in the range from 0 to 180 deg.

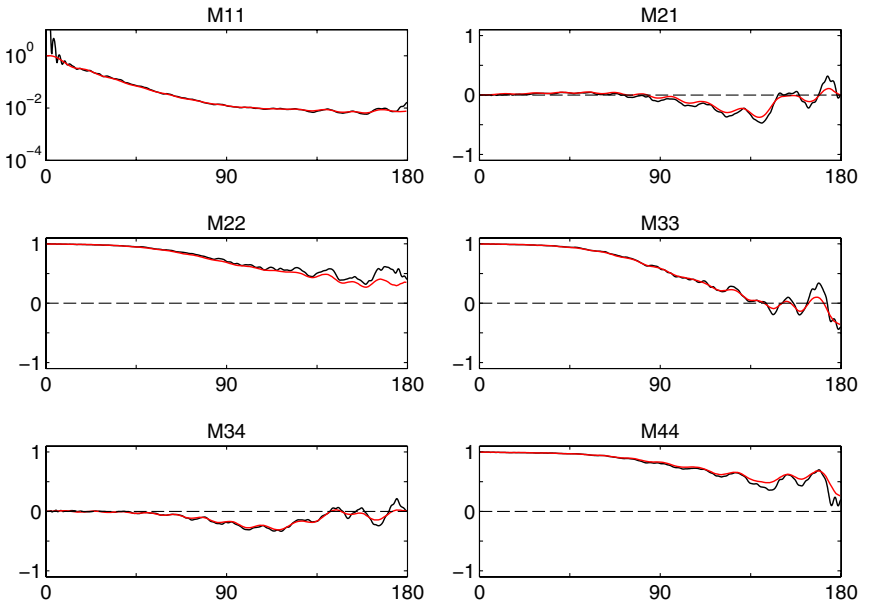

Fig. 4 Relevant Müller matrix elements for $N = 48$ nonabsorbing spheres ($f_V = 20.11$ Vol.-%). All elements are normalized to M_{11}, the M_{11} element is normalized to forward direction. Every element is depicted versus the scattering angle θ in the range from 0 to 180 deg. Increasing deviations due to dependent scattering can be observed.

M_{34} are shown in Fig. 3 (12 spheres), Fig. 4 (48 spheres) and Fig. 5 (96 spheres).

3.1 *Effects on Multiple and Dependent Scattering*

This study was aimed at pointing out agreements and differences between the two light scattering simulation approaches for polarized light. It can be observed that especially for small concentrations the two methods are in good agreement for all Müller matrix elements. This was already described for unpolarized light[27] and was now observed for polarized light within this study.[28] With increasing scatterer concentrations slightly increasing differences can be observed for all Müller matrix elements, mainly for higher scattering angles. These differences are attributed to dependent scattering effects since multiple scattering is considered by both solution methods. In Fig. 6 the angular errors are depicted for the same Müller matrix elements as above and three different volume concentrations. For M_{11} the relative error and for all normalized elements $i,j = 1, \ldots, 4$ the difference $M_{ij}^{GMM} - M_{ij}^{\mathrm{MonteCarlo}}$ between the both methods is shown. Only for large investigated volume concentrations above 20 Vol.-% dependent scattering effects become predominant, especially in the backscattering hemisphere. It is not possible to reproduce dependent scattering by standard solutions of the radiative transfer theory due to

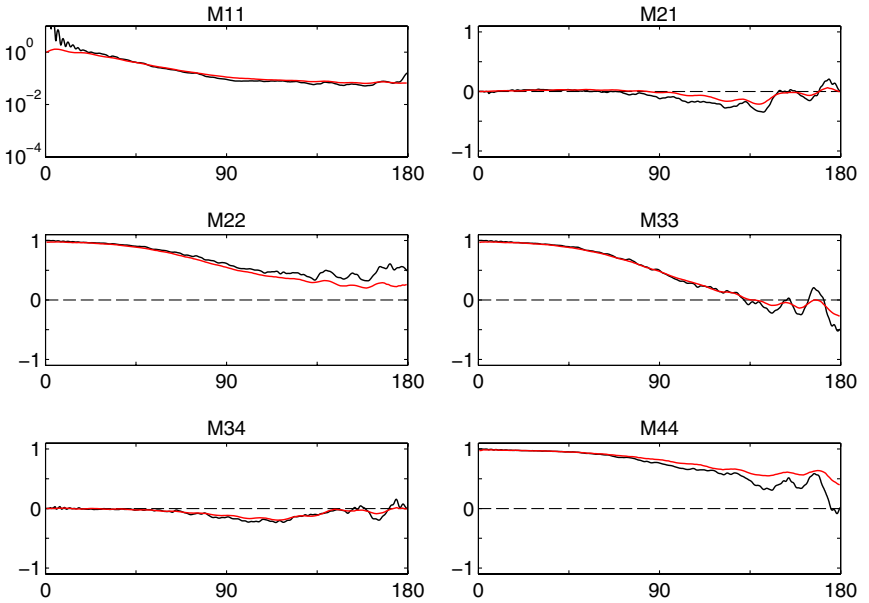

Fig. 5 Relevant Müller matrix elements for $N = 96$ nonabsorbing spheres ($f_V = 40.21$ Vol.-%). All elements are normalized to M_{11}, the M_{11} element is normalized to forward direction. Every element is depicted versus the scattering angle θ in the range from 0 to 180 deg. Deviations due to dependent scattering are obvious.

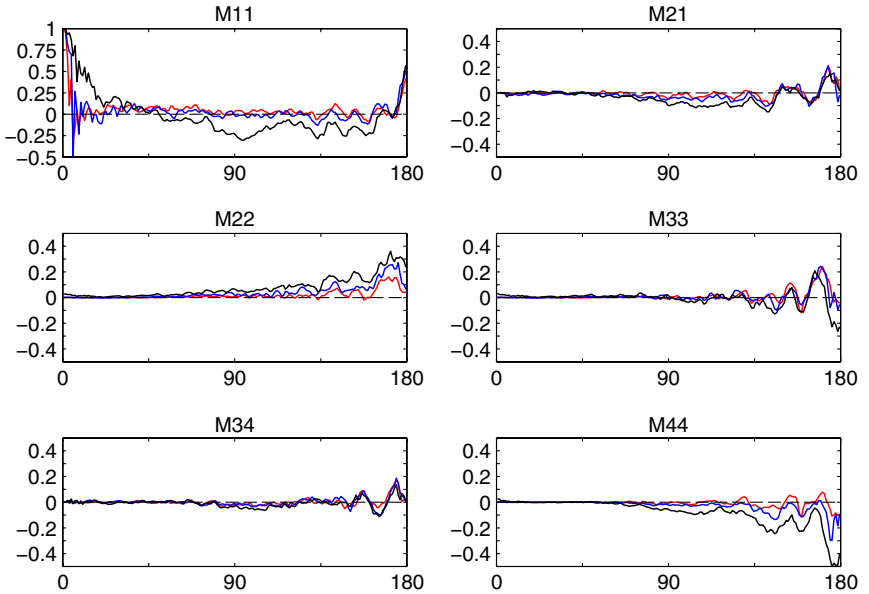

Fig. 6 Concentration dependent deviations between Maxwell and Monte Carlo results for all relevant Müller matrix elements. In case of M_{11} the relative error is calculated, otherwise the difference between normalized elements. For volume concentrations of $f_V = 10.05$ Vol.-% (red), $f_V = 20.11$ Vol.-% (blue) and $f_V = 40.21$ Vol.-% (black) the resulting deviations are depicted versus the scattering angle θ in the range from 0 to 180 deg. Apart from forward- and backscattering peaks ($\theta \approx 20 - 170$ deg) deviations do not exceed 30%.

near field interactions. This has to be kept in mind whenever results of Monte Carlo simulations of polarized light propagation are regarded.

All Müller matrix elements show oscillations in the whole angular range, especially for small concentrations, while the oscillations are decreasing with increasing scatterer concentrations. These oscillations for small concentrations result from the solution of scattering by a single sphere (Mie scattering). With increasing concentrations, multiple scattering becomes predominant which leads to a reduction of the oscillation amplitudes.

3.2 *Results for the Unpolarized Intensity*

The M_{11} element is a normalized measure for the scattered intensity for unpolarized light. The differences in the M_{11} element between the two methods for small angles ($\theta \lesssim 10$ deg) are due to forward interferences resulting from the limited simulation volume (Maxwell theory).[27] The angular width of these forward interferences would become infinitesimally small if a laterally infinite instead of a finite cubic simulation volume would be regarded. Another effect is the coherent backscattering peak[43] at $\theta \asymp 180$ deg which can be reproduced by Maxwell

theory in contrast to the radiative transfer theory. It can be observed for all concentrations and for scattering angles θ near 180 deg and becomes more pronounced for high scatterer concentrations. Forward interferences and coherent backscattering cannot be reproduced by the Monte Carlo method as the radiative transfer theory neglects the wave character of light.

Beside that, it can be observed that the angular distribution of the M_{11} element flattens for higher sphere numbers, i.e., the scattered intensity becomes more isotropic with increasing concentrations. This effect appears for both methods. Further, a flattening of the oscillations attributed to the single Mie scattering function is found for higher concentrations, also for the other Müller matrix elements. Increasing concentrations lead to irregular deviations of the M_{11} element between both methods being most apparent for the highest concentration (96 spheres). The Monte Carlo solution stays rather smooth while the exact Maxwell results show more oscillations, even if no speckles are considered.

3.3 *Polarization Specific Müller Matrix Elements*

The absolute value of all normalized Müller matrix elements (except M_{11}) generally decreases for higher angles as the concentration increases. This effect, investigated with Monte Carlo simulations, was attributed to multiple scattering by Tuchin et al.[6] The Maxwell solutions presented here show a similar behavior even if increasing deviations to the Monte Carlo solutions for higher concentrations are taken into account. The decrease of these Müller matrix elements indicates the depolarizing character of multiple scattering. It is important to mention that the described decrease is mostly present, though for some angles there are also exceptions of this behavior.

For angles near forward direction, the M_{22}, M_{33} and M_{44} elements take values near 1, while the off-diagonal elements take values near 0 for all concentrations. This means that the polarization properties are better maintained in the forward direction. For both simulation methods this effect is dominant for small concentrations.

The M_{44} element contains information about the circular polarization. It also decreases when scatterer concentrations increase for forward scattering angles $\theta \lesssim 50$ deg, but the decrease is smaller than for the M_{22} and M_{33} Müller matrix elements. For higher scattering angles, no general decrease with higher concentrations of the M_{44} element can be observed from the Monte Carlo simulations. It could be confirmed that this effect can mainly be attributed to multiple scattering as was assumed by Maksimova et al.,[18] who considered constant scatterer concentrations (size parameters in the Mie regime), but increasing scattering volumes. This may indicate that circular polarization is better maintained than linear polarization for multiple scattering. However, for very high scatterer concentrations as is the case for 96 spheres dispersed in the medium it can be observed (see Fig. 5) that the M_{44} element calculated by Maxwell theory is below the M_{44} element calculated by the Monte Carlo method while the M_{22} element shows an opposite behavior. This shows that the better maintenance of circular polarization for high scatterer concentrations is not as manifest as could be expected only due to multiple scattering. In this case dependent scattering leads to a further reduction of the M_{44} element. It has to be mentioned that these results hold for the parameters used in this study with scatterers in the Mie regime and a relatively high refractive index mismatch between scatterer and surrounding medium. For scattering media in the Rayleigh regime or in the Mie regime in case of scatterers with low relative refractive index it is possible that linear polarization is better maintained than circular polarization.[5]

4 Conclusions

In summary it could be shown that it is possible to reproduce the exact Maxwell solutions for low to moderate volume concentrations in good approximation when using a polarization sensitive Monte Carlo code based on radiative transfer theory. This holds for all Müller matrix elements, especially for scattering angles $\theta \lesssim 140$ deg. For high volume concentrations of the scatterers ($\gtrsim$20 Vol.-% in this study), dependent scattering effects are no longer negligible, so in case of highly concentrated scatterers the results of the Monte Carlo method must be taken with care, especially for high scattering angles.

The direct comparison method between solutions of the radiative transfer theory and Maxwell theory for the whole Müller matrix is useful for testing polarization dependent Monte Carlo programs for arbitrary optical properties of the scatterers and the surrounding medium. This could lead to more realistic simulation models of biological tissue. An extended investigation for complex models including polydisperse and absorbing scatterers, as is the case for biological media, is expected to disclose more polarization features.

Acknowledgments

We acknowledge support of the Deutsche Forschungsgemeinschaft (DFG grant KI 538/14-1).

References

1. H. Ding et al., "Angle-resolved Mueller matrix study of light scattering by B-cells at three wavelengths of 442, 633, and 850 nm," *J. Biomed. Opt.* **12**(03), 034032 (2007).
2. Y. Liu et al., "Optical markers in duodenal mucosa predict the presence of pancreatic cancer," *Clin. Cancer Res.* **13**(15), 4392–4399 (2007).
3. J. C. Ramella-Roman, A. Nayak, and S. A. Prahl, "Spectroscopic sensitive polarimeter for biomedical applications," *J. Biomed. Opt.* **16**(04), 047001 (2011).
4. B. V. Bronk et al., "Measuring diameters of rod-shaped bacteria in vivo with polarized light scattering," *Biophys. J.* **69**(3), 1170–1177 (1995).
5. N. Ghosh and I. Vitkin, "Tissue polarimetry: concepts, challenges, applications, and outlook," *J. Biomed. Opt.* **16**(11), 110801 (2011).
6. V. Tuchin, L. Wang, and D. Zimnyakov, *Optical Polarization in Biomedical Applications*, Vol. **1**, Springer, Berlin (2006).
7. C. Chu and S. Churchill, "Multiple scattering by randomly distributed obstacles—methods of solution," *IEEE Trans. Antenn. Propag.* **4**(2), 142–148 (1956).
8. B. Wilson and G. Adam, "A Monte Carlo model for the absorption and flux distributions of light in tissue," *Med. Phys.* **10**(6), 824–830 (1983).
9. M. Antonelli et al., "Mueller matrix imaging of human colon tissue for cancer diagnostics: how Monte Carlo modeling can help in the interpretation of experimental data," *Opt. Express* **18**(10), 10200–10208 (2010).
10. S. Bartel and A. Hielscher, "Monte Carlo simulations of the diffuse backscattering Mueller matrix for highly scattering media," *Appl. Opt.* **39**(10), 1580–1588 (2000).
11. B. Cameron, Y. Li, and A. Nezhuvingal, "Determination of optical scattering properties in turbid media using Mueller matrix imaging," *J. Biomed. Opt.* **11**(05), 054031 (2006).
12. A. Hielscher et al., "Diffuse backscattering Mueller matrices of highly scattering media," *Opt. Express* **1**(13), 441–453 (1997).
13. M. J. Raković et al., "Light backscattering polarization patterns from turbid media: theory and experiment," *Appl. Opt.* **38**(15) 3399–3408 (1999).
14. H. Akarçay and J. Ricka, "Simulating light propagation: towards realistic tissue models," *Proc. SPIE* **8088**(1), 80880K (2011).

15. D. Côté and I. Vitkin, "Robust concentration determination of optically active molecules in turbid media with validated three-dimensional polarization sensitive Monte Carlo calculations," *Opt. Express* **13**(1), 148–163 (2005).
16. X. Guo, M. Wood, and A. Vitkin, "A Monte Carlo study of penetration depth and sampling volume of polarized light in turbid media," *Opt. Commun.* **281**(3), 380–387 (2008).
17. G. Kattawar and C. Adams, "Stokes vector calculations of the submarine light field in an atmosphere-ocean with scattering according to a Rayleigh phase matrix: effect of interface refractive index on radiance and polarization," *Limnol. Oceanogr.* **34**(8), 1453–1472 (1989).
18. I. L. Maksimova, S. Romanov, and V. Izotova, "The effect of multiple scattering in disperse media on polarization characteristics of scattered light," *Opt. Spectrosc. (USSR)* **92**(6), 915–923 (2002).
19. M. Xu, "Electric field Monte Carlo simulation of polarized light propagation in turbid media," *Opt. Express* **12**(26), 6530–6539 (2004).
20. J. Ramella-Roman, S. Prahl, and S. Jacques, "Three Monte Carlo programs of polarized light transport into scattering media: part I," *Opt. Express* **13**(12), 4420–4438 (2005).
21. X. Wang and L. Wang, "Propagation of polarized light in birefringent turbid media: a Monte Carlo study," *J. Biomed. Opt.* **7**(3), 279–290 (2002).
22. A. Taflove and S. Hagness, "Computational electrodynamics: the finite-difference time-domain method," *Artech House Antennas and Propagation Library* Artech House, Boston (2005).
23. B. Draine and P. Flatau, "Discrete-dipole approximation for scattering calculations," *JOSA A* **11**(4), 1491–1499 (1994).
24. S. H. Tseng and B. Huang, "Comparing Monte Carlo simulation and pseudospectral time-domain numerical solutions of Maxwell's equations of light scattering by a macroscopic random medium," *Appl. Phys. Lett.* **91**(5), 051114 (2007).
25. J. Schäfer and A. Kienle, "Scattering of light by multiple dielectric cylinders: comparison of radiative transfer and Maxwell theory," *Opt. Lett.* **33**(20), 2413–2415 (2008).
26. L. Roux et al., "Scattering by a slab containing randomly located cylinders: comparison between radiative transfer and electromagnetic simulation," *JOSA A* **18**(2), 374–384 (2001).
27. F. Voit, J. Schäfer, and A. Kienle, "Light scattering by multiple spheres: comparison between Maxwell theory and radiative-transfer-theory calculations," *Opt. Lett.* **34**(17), 2593–2595 (2009).
28. A. Hohmann et al., "Comparison of Monte Carlo simulations of polarized light propagation in turbid media with exact Maxwell solutions," *Proc. SPIE* **8090**(1), 80900H (2011).
29. A. Kienle et al., "Light propagation in dentin: influence of microstructure on anisotropy," *Phys. Med. Biol.* **48**(2), N7–N14 (2003).
30. Y. Xu, "Electromagnetic scattering by an aggregate of spheres," *Appl. Opt.* **34**(21), 4573–4588 (1995).
31. J. Hovenier, "Structure of a general pure Mueller matrix," *Appl. Opt.* **33**(36), 8318–8324 (1994).
32. C. Bohren and D. Huffman, *Absorption and Scattering of Light by Small Particles*, Wiley-Interscience, New York (1998).
33. G. Mie, "Beiträge zur Optik trüber Medien, speziell kolloidaler Metallösungen," *Ann. Phys.* **330**(3), 377–445 (1908).
34. Y. Xu and B. Gustafson, "An analytical solution to electromagnetic multisphere-scattering," Technical Report, Department of Astronomy, University of Florida (2003) available at: http://www.scattport.org/files/xu/codes.htm.
35. Y. Xu, "Scattering Mueller matrix of an ensemble of variously shaped small particles," *JOSA A* **20**(11), 2093–2105 (2003).
36. N. Metropolis et al., "Equation of state calculations by fast computing machines," *J. Chem. Phys.* **21**(6), 1087–1092 (1953).
37. L. Tsang et al., *Scattering of Electromagnetic Waves: Numerical Simulations*, Wiley-Interscience, New York, Vol. **2** (2001).
38. H. Van de Hulst, *Light scattering by Small Particles*, Dover Publications, New York, Vol. **1** (1981).
39. M. Hofer and O. Glatter, "Mueller matrix calculations for randomly oriented rotationally symmetric objects with low contrast," *Appl. Opt.* **28**(12), 2389–2400 (1989).
40. M. Mishchenko and D. Mackowski, "Coherent backscattering in the cross-polarized channel," *Phys. Rev. A* **83**(1), 013829 (2011).
41. S. Savenkov, "Mueller-matrix characterization of biological tissues," *Polarimetric Detection, Characterization and Remote Sensing*, NATO Science for Peace and Security Series C: Environmental Security Series, Springer, Dordrecht, pp. 437–472 (2011).
42. D. Bicout et al., "Depolarization of multiply scattered waves by spherical diffusers: influence of the size parameter," *Phys. Rev. E* **49**(2), 1767–1770 (1994).
43. M. Mishchenko, L. Travis, and A. Lacis, *Multiple Scattering of Light by Particles: Radiative Transfer and Coherent Backscattering*, Cambridge Univ. Press, New York (2006).